Control of a Three-Phase Power Converter Connected to Unbalanced Power Grid in a Non-Cartesian Oblique Frame

Grzegorz Iwanski , *Senior Member, IEEE*, Sebastian Wodyk , and Tomasz Luszczyk

Abstract—The article presents a new approach to positive and negative sequence current vector control of a grid-connected three-phase three-wire power electronic converter operating under grid voltage imbalance conditions. The concept utilizes the representation of unbalanced converter current in the new coordinates frame in which the current vector components are constant. The nonlinear trigonometric transformation of two-dimensional current vector components from the stationary frame to the new frame is found online depending on the reference current asymmetry. The presented concept of new coordinates utilization allows implementation of proportional-integral terms as current regulators without the use of resonant terms and without the use of the measured current symmetrical sequences decomposition. The article presents the theoretical approach, simulation results, as well as laboratory tests results.

Index Terms—AC–DC power conversion, current control, Clarke's transformation, Park's transformation.

NOMENCLATURE

x	General vector representing any three-phase signal (voltage, current, and possibly flux in an electric machine).
x_a, x_b, x_c	General three-phase signals.
$|x_a|, |x_b|, |x_c|$	Amplitudes of *abc* three-phase general signals.
x_α, x_β	$\alpha\beta$ components of the general vector in a classic stationary frame obtained by the Clarke transformation.
$x_\alpha{}^d, x_\beta{}^d, x_\alpha{}^q, x_\beta{}^q$	Direct (^{d}) and quadrature (^{q}) components of general vector $\alpha\beta$ components.
$|x_\alpha|, |x_\beta|$	Amplitudes of classic $\alpha\beta$ stationary frame components of the general vector.
$x_{\alpha p}, x_{\beta p}, x_{\alpha n}, x_{\beta n}$	$\alpha\beta$ components of the general vector positive and negative sequence in a classic stationary frame.
$x_\alpha{}', x_\beta{}'$	$\alpha\beta$ components of the general vector in a modified non-Cartesian stationary frame obtained with the new transformation.
$|x_\alpha{}'|, |x_\beta{}'|$	Amplitudes of new non-Cartesian $\alpha\beta$ stationary frame components of the general vector.
x_d, x_q	*dq* components of the general vector in a classic rotating frame obtained with Park's rotation transformation.
$x_{dp}, x_{qp}, x_{dn}, x_{qn}$	*dq* components of the general vector positive and negative sequence in a classic stationary frame.
$x_{dp}{}^t, x_{qp}{}^t, x_{dn}{}^t, x_{qn}{}^t$	*dq* components of the general vector positive and negative sequence in a classic stationary frame used for transformation parameters determination after consideration of dead zones.
$|x_p|, |x_n|$	Positive and negative sequence vector lengths.
$x_d{}', x_q{}'$	*dq* components of the general vector in a modified non-Cartesian rotating frame obtained with the new transformation and Park's rotation transformation.
$|x_{abc}|^{\max}$	Maximum amplitude from among amplitudes of phase general signals.
$|x|_{\text{base}}$	Base amplitude for the new transformation (base vector length giving the new transformation output signals amplitudes equal to $|x|_{\text{base}}$).
a, b, c, d	New non-Cartesian transformation factors.
θ_s	Synchronous angle (transformation angle for Park's transformation) calculated on the basis of positive sequence $\alpha\beta$ fundamental frequency components.

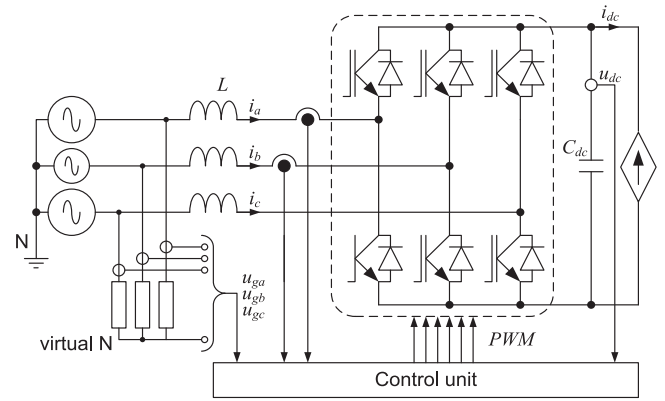| u_g	Grid voltage vector.
u_{ga}, u_{gb}, u_{gc}	Grid voltage vector three-phase signals.
$u_{g\alpha}, u_{g\beta}$	Grid voltage vector $\alpha\beta$ components in a classic stationary frame obtained by the Clarke transformation.
$u_{g\alpha}{}^d, u_{g\beta}{}^d, u_{g\alpha}{}^q, u_{g\beta}{}^q$	Grid voltage vector direct (^{d}) and quadrature (^{q}) components in the stationary $\alpha\beta$ frame.
$u_{g\alpha p}, u_{g\beta p}, u_{g\alpha n}, u_{g\beta n}$	Grid voltage vector positive and negative sequence components in the stationary $\alpha\beta$ frame.
$\lvert u_{gp} \rvert$	Actual grid voltage positive sequence vector length.
$\lvert u_{gp} \rvert^{\text{ref}}$	Reference grid voltage positive sequence vector length.
u_{gdn}, u_{gqn}	Actual grid voltage negative sequence vector components in the counter-rotating dq frame.
$u_{gdn}{}^{\text{ref}}, u_{gqn}{}^{\text{ref}}$	Reference grid voltage negative sequence vector components in the counter-rotating dq frame.
$i-$	Converter current vector.
i_α, i_β	Actual $\alpha\beta$ components of the converter current vector in a classic stationary frame.
$i_\alpha{}^{\text{ref}}, i_\beta{}^{\text{ref}}$	Reference $\alpha\beta$ components of the converter current vector in a classic stationary frame.
$i_\alpha{}', i_\beta{}'$	Actual $\alpha'\beta'$ components of the converter current vector in a new non-Cartesian stationary frame.
$i_\alpha{}'^{\text{ref}}, i_\beta{}'^{\text{ref}}$	Reference $\alpha'\beta'$ components of the converter current vector in a new non-Cartesian stationary frame.
$i_{dp}{}^{\text{ref}}, i_{qp}{}^{\text{ref}}, i_{dn}{}^{\text{ref}}, i_{qn}{}^{\text{ref}}$	Reference dq components of the positive and negative sequence converter current vector in a classic rotating frame.
$\varepsilon_{ia}{}', \varepsilon_{ib}{}'$	Control errors of the current vector components regulation in a new non-Cartesian stationary frame.
u_{ca}, u_{cb}, u_{cc}	Three-phase converter voltage.
i_{dc}	DC loading/sourcing current.
u_{dc}	Actual dc voltage.
$u_{dc\cdot avg}$	Average value of the actual dc voltage.
$u_{dc}{}^{\text{ref}}$	Reference dc voltage.
$R-$	Grid filter resistance.
$L-$	Grid filter inductance.
C_{dc}	DC bus capacitance.
$T_{\alpha'\beta'}$	New transformation from classic $\alpha\beta$ stationary frame to the new $\alpha'\beta'$ stationary frame.
$T_{\alpha'\beta'}{}^{-1}$	Inverse transformation from the new $\alpha'\beta'$ stationary frame to the classic $\alpha\beta$ stationary frame.

Fig. 1. Scheme of the power circuit of a three-phase power electronic converter operating with unbalanced grid voltage.

$outRi_d{}', outRi_q{}'$	Output signals of current vector components regulators.

I. INTRODUCTION

POWER electronics converters used as grid interfaces between energy sources, energy storage systems, and loads can nowadays be treated as a mature technology. Mostly they are used as single-phase systems for fractional power and three-phase systems for kilowatt range and above. A scheme of the three-phase power electronics converter operating with a three-phase three-wire grid under grid voltage imbalance is shown in Fig. 1. Some recent grid codes take into consideration assistance of energy conversion systems in the field of negative sequence management during asymmetrical grid voltage sags aiming at power system stability increase and improvement of energy quality [1].

A crucial issue for positive and negative sequences management without additional current distortions is a converter current control loop. Both sufficient dynamics of converter current control and adequate nondistorted reference current vector components signals are equally important. Basically, two manners are used for current control. The first one utilizes the decomposition of sequences with separate coordinates frames and proportional-integral (PI) current regulators for each sequence [2]. The second one utilizes proportional-resonant (PR) terms as current vector component controllers in the abc frame [3] or in the stationary $\alpha\beta$ frame [4], [5], or PI-resonant (PIR) controllers in a rotating frame [6].

The sequence decomposition-based classic double synchronous reference frame (DSRF) control [7] requires notch filters deteriorating the dynamics of current control loops. This is why more sophisticated DSRFs with decoupling terms between positive and negative sequence control paths [8] are developed. The DSRF-based control method simplifies the issue of current controllers state limitation and simultaneous control signal limitation due to the applied PI term in each of the four control paths. However, another issue—limitation of total reference converter current at an appropriate level—has to be solved, which for unbalanced current targets is not obvious. The improved structures of DSRF control still require sophisticated structures of precise limitation of phase current, but what is more

important, a number of trigonometric functions calculations for rotation transformation in the main paths and in decoupling paths.

For unbalanced sinusoidal phase current limitation, some sophisticated methods are applied, which require a number of calculations [9], therefore other methods of reference signals calculation matching the desired control targets, without sequences decomposition, are developed [10], [11]. However, the resonant terms are used to track the reference current. Digital implementation of resonant terms is not complicated when some rules are kept (e.g., prewarping in discretization [12]). However, they need associated structures of state limitation (antiwind-up), which are more complicated than PI controllers and not so intuitive.

To limit the state of oscillatory signals, simple cutting can be made [13], but then the output signals are no longer sinusoidal. To keep the sinusoidal character of resonant terms output signals, an adaptation of the damping factor is applied when the signal exceeds the limit [14]. The damping factor is changed by an additional controller (e.g., a proportional one with a high gain). An additional term influencing the damping factor requires a separate tuning procedure, and it makes the tuning (selection of gains) of the whole structure not trivial. Parallel operation of resonant terms to the others (such as integral terms in the PIR regulator in control realized in a rotating frame) causes anti-windup structures even more complex, especially when more than one variable is under control [15].

This article presents a new approach of three-phase three-wire converter control using transformation to the non-Cartesian frame. The parameters of transformation to the new frame are selected to obtain sinusoidal signals in the new stationary frame with the same amplitude and shifted by $\pi/2$. Thus, after next Park's transformation to the new rotating frame, the signals are constant. This allows the implementation of two control paths with PI controllers instead PR-integral or four control paths in DSRF. To obtain such a result of transformation for any imbalance of the referenced converter current, the transformation parameters are calculated on the basis of positive and negative reference current components.

Such a manner is already applied in post-fault control of multiphase machines [16] or even in three-phase machines fed from a four-wire power converter [17]. The difference is that in the electric machine, the transformations parameters can be calculated offline depending on the type of fault and mapped in a table. For a grid converter, new transformation parameters are calculated in real-time, because reference current asymmetry is generally not arbitrarily set.

A similar concept to the one presented in this article is described in [18] and [19]. The presented concept introduces transformation from the natural *abc* system to the new $\alpha'\beta'$ frame in which the transformed signals are balanced. The transformation parameters are calculated based on the phase voltage measurement in the three-phase system. Thus, there are more transformation parameters to find and the method of calculation using trigonometric functions is more complicated. Additionally, using the presented approach, the selected transformation is adequate for the current asymmetry corresponding to the grid

voltage asymmetry. The second control target (current asymmetry opposite to the grid voltage asymmetry) requires new derivation and recalculation of the transformation parameters, but in such case, additionally, the disturbance rejection structure (grid voltage feed-forward) must be moved to the other part of the control structure.

The solution for current corresponding asymmetry, full symmetry, and opposite asymmetry, with the adequate placing of grid voltage feed-forward is presented in [20], in which instead of the *abc* to $\alpha'\beta'$ frame transformation, the $\alpha\beta$ to $\alpha'\beta'$ transformation is used. There are only four transformation parameters that additionally are calculated in a simpler way without trigonometric functions, but are obtained using the definition of cross and dot products of respective direct and quadrature $\alpha\beta$ signals. However, the transformation parameters are calculated on the basis of the grid voltage vector components with a specific asymmetry factor, and the asymmetry of current other than asymmetry of voltage is difficult to obtain. Thus, the new approach of transformation is extended in this article to obtain current asymmetry different than grid voltage asymmetry also.

II. DERIVATION OF THE PROPOSED TRANSFORMATION

A. Direct Transformation

Representation of the three-phase three-wire system as a two-phase system can be made with Clarke's transformation [22], which in the case of no zero-sequence occurrence as it is measured in Fig. 1 can be simplified to the form

$$\begin{bmatrix} x_\alpha \\ x_\beta \end{bmatrix} = \begin{bmatrix} 1 & 0 & 0 \\ 0 & \frac{\sqrt{3}}{3} & -\frac{\sqrt{3}}{3} \end{bmatrix} \begin{bmatrix} x_a \\ x_b \\ x_c \end{bmatrix} \tag{1}$$

in which three-phase signals (such as three-phase voltage, three-phase current, or three-phase flux in an electric machine) x_a, x_b, and x_c are represented by two orthogonal components x_α and x_β of the vector x in a stationary frame. This transformation is valid for a vector x containing both positive and negative sequence components, and the vector $\alpha\beta$ components can be described as

$$x_\alpha = |x_\alpha| \cos(\theta_s - \theta_\alpha) \tag{2a}$$

$$x_\beta = |x_\beta| \cos(\theta_s - \theta_\beta) \tag{2b}$$

in which $|x_\alpha|$ and $|x_\beta|$ are amplitudes of $\alpha\beta$ components, and θ_α and θ_β are phase shifts between $\alpha\beta$ components and positive sequence α component, respectively.

Park's transformation [23] allows the representation of vector x containing only a positive sequence component by constant values in a rotating frame. However, for the vector containing positive and negative sequences, x_d and x_q components of the vector, besides dc components, contain double grid frequency oscillatory components, which require more sophisticated controllers than PI terms. This is why the proposed approach is elaborated, in which *dq* components are represented in a new frame, in which these components are constant (i.e., without oscillatory components). To achieve this target, a new $\alpha'\beta'$ stationary frame is found as first, in which stationary frame

components have the same amplitudes and are shifted by $\pi/2$. Thus, after transformation to the new dq frame rotating with the synchronous angle, the new $d'q'$ components would be constant.

Let us assume that there exists a nonlinear transformation to the new stationary $\alpha'\beta'$ frame providing that new components x'_α and x'_β are shifted by $\pi/2$ and both component amplitudes equal the base amplitude $|x|_{\text{base}}$, which is selected as maximum among phase signals amplitudes. The new components x'_α and x'_β are described by

$$x'_\alpha = |x|_{\text{base}} \ \cos\theta_s \tag{3a}$$

$$x'_\beta = |x|_{\text{base}} \ \sin\theta_s. \tag{3b}$$

The transformation from $\alpha\beta$ to the new $\alpha'\beta'$ takes the general form

$$\begin{bmatrix} x'_\alpha \\ x'_\beta \end{bmatrix} = \mathbf{T}_{\alpha'\beta'} \ \begin{bmatrix} x_\alpha \\ x_\beta \end{bmatrix} = \begin{bmatrix} a & b \\ c & d \end{bmatrix} \begin{bmatrix} x_\alpha \\ x_\beta \end{bmatrix}. \tag{4}$$

The transformation factors $abcd$ can be found based on the values of positive x_{dqp} and negative x_{dqn} sequence components. When the asymmetry of the transformed signals is freely adjusted like current asymmetry in the grid power converter, the transformation parameters can be determined on the basis of the positive and negative sequence components x_{dp}, x_{qp}, x_{dn}, and x_{qn} referenced in each of the four parallel control paths.

The positive and negative sequence $\alpha\beta$ components in a classic stationary frame can be calculated as

$$\begin{bmatrix} x_{\alpha p} \\ x_{\beta p} \end{bmatrix} = \begin{bmatrix} \cos\theta_s & -\sin\theta_s \\ \sin\theta_s & \cos\theta_s \end{bmatrix} \begin{bmatrix} x_{dp} \\ x_{qp} \end{bmatrix} \tag{5a}$$

$$\begin{bmatrix} x_{\alpha n} \\ x_{\beta n} \end{bmatrix} = \begin{bmatrix} \cos\theta_s & \sin\theta_s \\ -\sin\theta_s & \cos\theta_s \end{bmatrix} \begin{bmatrix} x_{dn} \\ x_{qn} \end{bmatrix} \tag{5b}$$

and total x_α and x_β can be further calculated as

$$x_\alpha = x_{\alpha p} + x_{\alpha n} = (x_{dp} + x_{dn}) \cos\theta_s - (x_{qp} - x_{qn}) \sin\theta_s \tag{6a}$$

$$x_\beta = x_{\beta p} + x_{\beta n} = (x_{dp} - x_{dn}) \sin\theta_s + (x_{qp} + x_{qn}) \cos\theta_s. \tag{6b}$$

Inserting (3) and (6) into (4), each of the new $\alpha'\beta'$ equations can be rewritten:

$$|x|_{\text{base}} \ \cos\theta_s$$
$$= a\left((x_{dp} + x_{dn}) \cos\theta_s - (x_{qp} - x_{qn}) \sin\theta_s\right)$$
$$+ b\left((x_{dp} - x_{dn}) \sin\theta_s + (x_{qp} + x_{qn}) \cos\theta_s\right) \tag{7a}$$

$$|x|_{\text{base}} \ \sin\theta_s$$
$$= c\left((x_{dp} + x_{dn}) \cos\theta_s - (x_{qp} - x_{qn}) \sin\theta_s\right)$$
$$+ d\left((x_{dp} - x_{dn}) \sin\theta_s + (x_{qp} + x_{qn}) \cos\theta_s\right). \tag{7b}$$

There exists an infinite number of $a - b$ and $c - d$ pairs that meet (7). However, taking into account that (2) and (3) are time dependent (because θ_s is time dependent), finding the transformation factors $abcd$ time independent for a given asymmetry of the original vector x, can be done using two selected conditions.

Formulating (7) for specific angles of the synchronous vector (e.g., for $\theta_s = 0$, $\theta_s = \pi/2$)

$$\left. \begin{aligned} |x|_{\text{base}} &= a\,(x_{dp} + x_{dn}) + b\,(x_{qp} + x_{qn}) \\ 0 &= c\,(x_{dp} + x_{dn}) + d\,(x_{qp} + x_{qn}) \end{aligned} \right|_{\theta_s = 0} \tag{8a}$$

$$\left. \begin{aligned} 0 &= -a\,(x_{qp} - x_{qn}) + b\,(x_{dp} - x_{dn}) \\ |x|_{\text{base}} &= -c\,(x_{qp} - x_{qn}) + d\,(x_{dp} - x_{dn}) \end{aligned} \right|_{\theta_s = \pi/2} \tag{8b}$$

the transformation parameters can be derived as

$$a = (x_{dp} - x_{dn}) \ \frac{|x|_{\text{base}}}{|x_p|^2 - |x_n|^2} \tag{9a}$$

$$b = (x_{qp} - x_{qn}) \ \frac{|x|_{\text{base}}}{|x_p|^2 - |x_n|^2} \tag{9b}$$

$$c = -(x_{qp} + x_{qn}) \ \frac{|x|_{\text{base}}}{|x_p|^2 - |x_n|^2} \tag{9c}$$

$$d = (x_{dp} + x_{dn}) \ \frac{|x|_{\text{base}}}{|x_p|^2 - |x_n|^2}. \tag{9d}$$

Finally, (4) can be written as

$$\begin{bmatrix} x'_\alpha \\ x'_\beta \end{bmatrix} = \frac{|x|_{\text{base}}}{|x_p|^2 - |x_n|^2} \begin{bmatrix} x_{dp} - x_{dn} & x_{qp} - x_{qn} \\ -x_{qp} - x_{qn} & x_{dp} + x_{dn} \end{bmatrix} \begin{bmatrix} x_\alpha \\ x_\beta \end{bmatrix} \tag{10}$$

which is the form of the natural stationary $\alpha\beta$ frame to new stationary $\alpha'\beta'$ frame transformation providing that new frame $\alpha'\beta'$ components have the same amplitudes equal to the highest amplitude from among three-phase signals and the components are shifted by $\pi/2$. The transformation parameters are calculated on the basis of given values of positive and negative sequence components of the unbalanced vector represented in the frames rotating with θ_s and $-\theta_s$ angle (synchronously and counter-synchronously with a positive-sequence vector).

To bring the vector to the $d'q'$ frame in which the x vector components are constant, the Park's rotation transformation is used. Both transformations from $\alpha\beta$ to $\alpha'\beta'$ and from $\alpha'\beta'$ to $d'q'$ frame result in following:

$$\begin{bmatrix} x'_d \\ x'_q \end{bmatrix} = \frac{|x|_{\text{base}}}{|x_p|^2 - |x_n|^2} \begin{bmatrix} \cos\theta_s & \sin\theta_s \\ -\sin\theta_s & \cos\theta_s \end{bmatrix}$$
$$\begin{bmatrix} x_{dp} - x_{dn} & x_{qp} - x_{qn} \\ -x_{qp} - x_{qn} & x_{dp} + x_{dn} \end{bmatrix} \begin{bmatrix} x_\alpha \\ x_\beta \end{bmatrix} \tag{11}$$

where

$$\cos\theta_s = \frac{x_{\alpha p}}{|x_p|} \tag{12a}$$

$$\sin\theta_s = \frac{x_{\beta p}}{|x_p|}. \tag{12b}$$

Using (12), the trigonometric functions calculation based on the θ_s angle determination can be avoided.

B. Inverse Transformation

Let us write transformation (10) as

$$k\, x'_{\alpha\beta} = \mathbf{T}_{\alpha'\beta'}\, x_{\alpha\beta} \tag{13}$$

where

$$k = \frac{|x_p|^2 - |x_n|^2}{|x|_{\text{base}}} \tag{14}$$

and $\mathbf{T}_{\alpha'\beta'}$ is a transformation matrix.

Wishing to find $x_{\alpha\beta}$ when $x'_{\alpha\beta}$ is known, we can write

$$x_{\alpha\beta} = k\mathbf{T}_{\alpha'\beta'}^{-1} x'_{\alpha\beta} \tag{15}$$

and

$$\mathbf{T}_{\alpha'\beta'}^{-1} = \frac{1}{\det\left(\mathbf{T}_{\alpha'\beta'}\right)}\,\mathbf{C^T} \tag{16}$$

where $\mathbf{C^T}$ as a transposed matrix of complements equals

$$\mathbf{C^T} = \begin{bmatrix} x_{dp} + x_{dn} & -x_{qp} + x_{qn} \\ x_{qp} + x_{qn} & x_{dp} - x_{dn} \end{bmatrix} \tag{17}$$

and

$$\det\left(\mathbf{T}_{\alpha'\beta'}\right) = |x_p|^2 - |x_n|^2. \tag{18}$$

The final form of the inverse transformation from non-Cartesian $\alpha'\beta'$ to the natural $\alpha\beta$ frame can be written as

$$\begin{bmatrix} x_\alpha \\ x_\beta \end{bmatrix} = \frac{1}{|x|_{\text{base}}} \begin{bmatrix} x_{dp} + x_{dn} & -x_{qp} + x_{qn} \\ x_{qp} + x_{qn} & x_{dp} - x_{dn} \end{bmatrix} \begin{bmatrix} x'_\alpha \\ x'_\beta \end{bmatrix}. \tag{19}$$

Transformation of the x' vector represented in the $d'q'$ frame to the natural $\alpha\beta$ needs two transformations – inverse Park's transformation from the $d'q'$ frame to new $\alpha'\beta'$ and next from non-Cartesian $\alpha'\beta'$ to natural $\alpha\beta$

$$\begin{bmatrix} x_\alpha \\ x_\beta \end{bmatrix} = \frac{1}{|x|_{\text{base}}} \begin{bmatrix} x_{dp} + x_{dn} & -x_{qp} + x_{qn} \\ x_{qp} + x_{qn} & x_{dp} - x_{dn} \end{bmatrix}$$
$$\begin{bmatrix} \cos\theta_s & -\sin\theta_s \\ \sin\theta_s & \cos\theta_s \end{bmatrix} \begin{bmatrix} x'_d \\ x'_q \end{bmatrix}. \tag{20}$$

The presented theoretical tool converts the two-phase signal from the Cartesian frame to the other non-Cartesian frame, in which axes are mutually obliquely oriented. The detailed properties of the transformation and detailed relations between axes of the old and new frames as well as detailed relations between vectors components and their lengths are shown in [23]. The transformation factors were calculated using alpha/beta voltage components and a limited number of current targets can be obtained, whereas in this article, the transformation factors are calculated based on the reference current positive and negative sequence components to obtain almost any state of current (excluding a very narrow range of dead zone). Independent of the form of the matrix and the way of parameters calculation, it is, in fact, a change of the frame from Cartesian to non-Cartesian, so the matrix, in fact, plays the role of transformation.

C. Limitation of the Proposed Transformation

The proposed transformation has a limitation if

$$|x_p|^2 - |x_n|^2 \approx 0 \tag{21}$$

because the denominator of the factor preceding the transformation is close to zero. This disturbs the actual (measured) signal transformation (10) to x'_α, x'_β. This is why the limitation on the transformation parameters calculation (dead zones) is imposed as follows:

$$\begin{cases} x^t_{dp} = x_{dp} \\ x^t_{qp} = x_{qp} \\ x^t_{dn} = x_{dn} \\ x^t_{qn} = x_{qn} \end{cases} \tag{22a}$$

$$\text{if } (0.9\,|x_p| < |x_n| \le |x_p|) \text{ then } \begin{cases} x^t_{dn} = 0.9 x_{dn}\left(\frac{|x_p|}{|x_n|}\right) \\ x^t_{qn} = 0.9 x_{qn}\left(\frac{|x_p|}{|x_n|}\right) \end{cases} \tag{22b}$$

$$\text{else if } (0.9\,|x_n| < |x_p| < |x_n|) \text{ then } \begin{cases} x^t_{dp} = 0.9 x_{dp}\left(\frac{|x_n|}{|x_p|}\right) \\ x^t_{qp} = 0.9 x_{qp}\left(\frac{|x_n|}{|x_p|}\right) \end{cases} \tag{22c}$$

$$\text{if } ((|x_p| + |x_n|) < 0.1\,|x_{\max}|) \text{ then } \begin{cases} \begin{bmatrix} x'_\alpha \\ x'_\beta \end{bmatrix} = \begin{bmatrix} x_\alpha \\ x_\beta \end{bmatrix}. \end{cases} \tag{22d}$$

Components x^t_{dp}, x^t_{qp}, x^t_{dn}, and x^t_{qn} are the new reference components and are used not only as reference values but also for the transformation terms calculation as well. Taking into account that some components change depending on the dead zone selection, new $|x_p|^t$ and $|x_n|^t$ are calculated to find the k factor preceding the transformation (10). The final direct (11) and inverse (20) transformation sets take the following form:

$$\begin{bmatrix} x'_d \\ x'_q \end{bmatrix} = \frac{|x|_{\text{base}}}{\left(|x_p|^t\right)^2 - \left(|x_n|^t\right)^2} \begin{bmatrix} \cos\theta_s & \sin\theta_s \\ -\sin\theta_s & \cos\theta_s \end{bmatrix} \begin{bmatrix} t_{11} & t_{12} \\ t_{21} & t_{22} \end{bmatrix} \begin{bmatrix} x_\alpha \\ x_\beta \end{bmatrix} \tag{23}$$

$$\begin{bmatrix} x_\alpha \\ x_\beta \end{bmatrix} = \frac{1}{|x|_{\text{base}}} \begin{bmatrix} t_{22} & -t_{12} \\ -t_{21} & t_{11} \end{bmatrix} \begin{bmatrix} \cos\theta_s & -\sin\theta_s \\ \sin\theta_s & \cos\theta_s \end{bmatrix} \begin{bmatrix} x'_d \\ x'_q \end{bmatrix} \tag{24}$$

where $t_{11} - t_{22}$ are the $\alpha\beta$ to $\alpha'\beta'$ transformation terms calculated as

$$t_{11} = x^t_{dp} - x^t_{dn} \tag{25a}$$

$$t_{12} = x^t_{qp} - x^t_{qn} \tag{25b}$$

$$t_{21} = -x^t_{qp} - x^t_{qn} \tag{25c}$$

$$t_{22} = x^t_{dp} + x^t_{dn} \tag{25d}$$

on the basis of the new positive and negative sequence components x^t_{dp}, x^t_{qp}, x^t_{dn}, and x^t_{qn} considering dead zones (22b,c,d). The calculation of transformation parameters in this way is avoided in a narrow range of signal's asymmetry, for which practical implementation may cause signals obtained

through transformation undefined due to the low denominator of factor k.

$|x|_{\text{base}}$ is selected as a maximum amplitude from among phase signals amplitudes

$$|x|_{\text{base}} = \max\left\{|x_a|, |x_b|, |x_c|\right\} = |x_{abc}|^{\max}. \quad (26)$$

As it will be shown in simulation and experimental results, such a selection is helpful in the achievement of true phase current limitation in the converter control method. The desired phase signal amplitudes $|x_a|$, $|x_b|$, $|x_c|$ can be calculated using the same reference values of x_{dp}^t, x_{qp}^t, x_{dn}^t, x_{qn}^t in the following way:

$$|x_a| = \sqrt{\left(|x_p|^t\right)^2 + \left(|x_n|^t\right)^2 + 2\left(x_{dp}^t x_{dn}^t - x_{qp}^t x_{qn}^t\right)} \quad (27a)$$

$$|x_b| = \sqrt{\begin{array}{c}\left(|x_p|^t\right)^2 + \left(|x_n|^t\right)^2 - x_{dp}^t x_{dn}^t \\ -\sqrt{3}\left(x_{qp}^t x_{dn}^t + x_{dp}^t x_{qn}^t\right) + x_{qp}^t x_{qn}^t\end{array}} \quad (27b)$$

$$|x_c| = \sqrt{\begin{array}{c}\left(|x_p|^t\right)^2 + \left(|x_n|^t\right)^2 - x_{dp}^t x_{dn}^t \\ +\sqrt{3}\left(x_{qp}^t x_{dn}^t + x_{dp}^t x_{qn}^t\right) + x_{qp}^t x_{qn}^t\end{array}}. \quad (27c)$$

D. Exemplary Case Study of Unbalanced Vector Representation in a New Frame

Case 1: Exemplary simulation results showing unbalanced three-phase signals transformation properties in the case in which the asymmetry factor is out of the dead zone are shown in Fig. 2. Reference signals x_{dp}^t, x_{qp}^t, x_{dn}^t, and x_{qn}^t are set arbitrarily with step changes. It can be seen that independent of the referenced asymmetry of three-phase signals, visible as different amplitudes and/or phase shift other than $\pi/2$ in x_α and x_β waveforms in the natural stationary $\alpha\beta$ frame, the signals x'_α and x'_β in the new stationary $\alpha'\beta'$ frame have the same amplitude and are shifted by $\pi/2$, so after Park's transformation signals, x'_d and x'_q in a new rotating $d'q'$ frame are constant. Thus, the assumptions and derivations provided in Section II-A are confirmed.

Case 2: An exemplary case study for the case in which the asymmetry factor crosses the dead zone is shown in Fig. 3. Two components x_{dp}^t and x_{qn}^t are linearly changed to achieve the variable asymmetry factor, whereas for simplicity two components x_{qp}^t and x_{dn}^t are set to zero. Independent of the referenced asymmetry, visible in the behavior of x_α and x_β waveforms in a natural stationary $\alpha\beta$ frame, after transformation to the new stationary $\alpha'\beta'$ frame signals, x'_α and x'_β have the same amplitude and are shifted by $\pi/2$. After Park's transformation to the new rotating $d'q'$ frame, the signals x'_d and x'_q are constant. When crossing the dead zone in a very narrow range of asymmetry, the transformation parameters are held. Thus, the asymmetry factor close to 1 meant as a ratio of the negative sequence vector component to the positive sequence vector component is not available. However, as it is visualized in Fig. 4, presenting the reference vector hodograph for this case, the dead zone is very narrow, and as it will be shown next in the converter control simulation and experimental
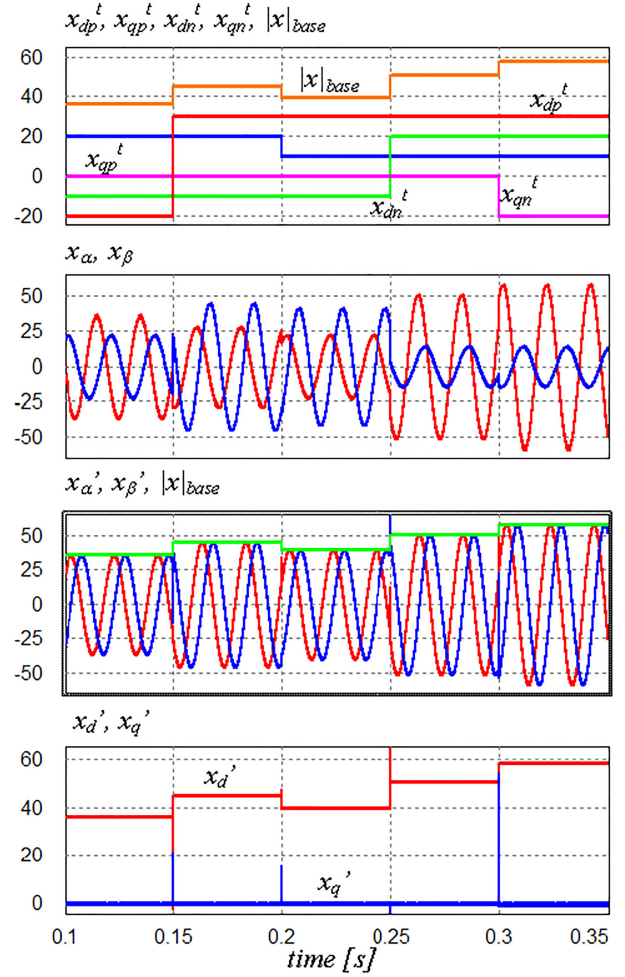

Fig. 2. Simulation results showing the new trigonometric transformation properties in the case in which the asymmetry factor is out of the dead zone.

tests, results do not considerably disturb the converter current waveforms.

III. CONTROL METHOD USING THE NEW TRANSFORMATIONS

A. Scheme of Voltage Vector Oriented Control Using the New Transformations

A control system allowing free management of the positive and negative sequence converter current vector depending on the dc load/source power and grid voltage conditions is shown in Fig. 5. Fig. 5(a) presents the main structure of voltage-oriented control with the new transformation.

The set of reference signals x_{dp}^t, x_{qp}^t, x_{dn}^t, and x_{qn}^t for transformation parameters $t_{11}-t_{22}$ calculation are identical to the reference current positive and negative sequence components i_{dp}^{ref}, i_{qp}^{ref}, i_{dn}^{ref}, i_{qn}^{ref} after consideration of dead zones. The reference currents i_{dp}^{ref}, i_{qp}^{ref}, i_{dn}^{ref}, i_{qn}^{ref} recalculated subsequently to the natural $\alpha\beta$ frame, next to the new $\alpha'\beta'$ frame, and by Park's transformation yield $i_d'^{\text{ref}} = |x|_{\text{base}}$ and $i_q'^{\text{ref}} = 0$ (the proof is provided in the Appendix). Thus, the reference current vector components may not be transformed by the set as above. The transformations are applied to the actual current vector
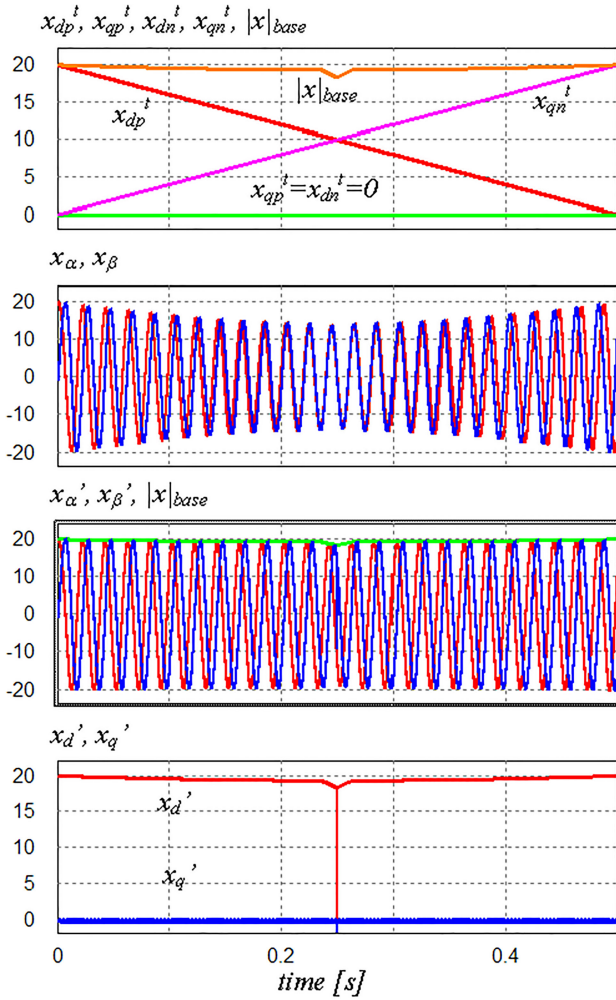
Fig. 3. Simulation results showing the new trigonometric transformation properties in the case in which the asymmetry factor crosses the dead zone.
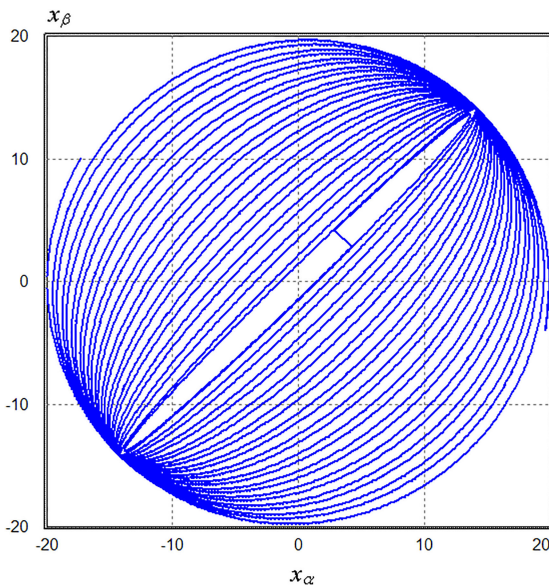

Fig. 4. Simulation results showing the reference vector hodograph in the case in which the asymmetry factor crosses the dead zone.

components $i_{\alpha\beta}$. The feedback is made for the new rotating frame $d'q'$ components of the current vector. Output signals of PI current vector components regulators are transformed back first using the inverse Park's transformation and next the inverse transformation from the new $\alpha'\beta'$ frame to the natural stationary $\alpha\beta$ frame. Afterwards, the grid voltage vector components feed-forward is applied, to reduce significantly an influence of the grid voltage vector disturbances on the converter current vector regulation. This manner is especially important during transients such as rapid symmetrical or asymmetrical voltage sags.

Fig. 5(b) presents the structure of determination of the grid voltage vector direct $u_{g\alpha}^d$ and $u_{g\beta}^d$ and quadrature $u_{g\alpha}^q$ and $u_{g\beta}^q$ components. The structure uses the set of second-order low-pass and high-pass filters with a cut-off frequency equal to 50 Hz. This method provides slightly better performance than another known method, which is second-order generalized integrator – used for direct and quadrature component derivation. The proof is provided in [9].

Direct $(u_{g\alpha}^d, u_{g\beta}^d)$ and quadrature $(u_{g\alpha}^q, u_{g\beta}^q)$ components of the grid voltage vector are used for further derivation of positive sequence voltage vector component amplitude $|u_{gp}|$, trigonometric functions of Park's transformation $(\sin\theta_s, \cos\theta_s)$ related to the positive sequence vector, and the dq components of negative sequence grid voltage vector components for their further compensation.

The exemplary outer control structures of dc voltage regulation and grid voltage imbalance correction are included in Fig. 5(a). The reader has to note that this part is exemplary and is not related to the main aim of this article, which is a new transformation for the current control structure. This part is only shown as an example of how to assign the reference value of positive and negative sequence current vector dq components. The actual dc voltage is filtered by second-order band-stop filter designed for 100-Hz central frequency and 40-Hz stopping band, and second-order low-pass filter designed for 150 Hz cut-off frequency. This is to avoid the influence of second and higher harmonics on the referencing of the i_{qp} component of current caused by the negative sequence current component and by possible harmonics in the grid voltage.

IV. SIMULATION RESULTS OF CONTROL METHODS WITH NON-CARTESIAN FRAME TRANSFORMATION

The first simulation tests are made to compare the two most popular current control methods for control of converter unbalanced current with the proposed solution utilizing the new transformation. Fig. 6(a) presents three-phase grid voltage of the following parameters: positive sequence phase voltage amplitude – 260 V, negative sequence phase voltage amplitude – 65 V, fifth harmonics amplitude – 32.5 V. Subsequent figures present the step response on the converter current asymmetry change: Fig. 6(b) for DSRF control with notch filters, Fig. 6(c) for DSRF control with decoupling structures between positive and negative sequence, Fig. 6(d) for resonant terms based control, and Fig. 6(e) for the proposed control.
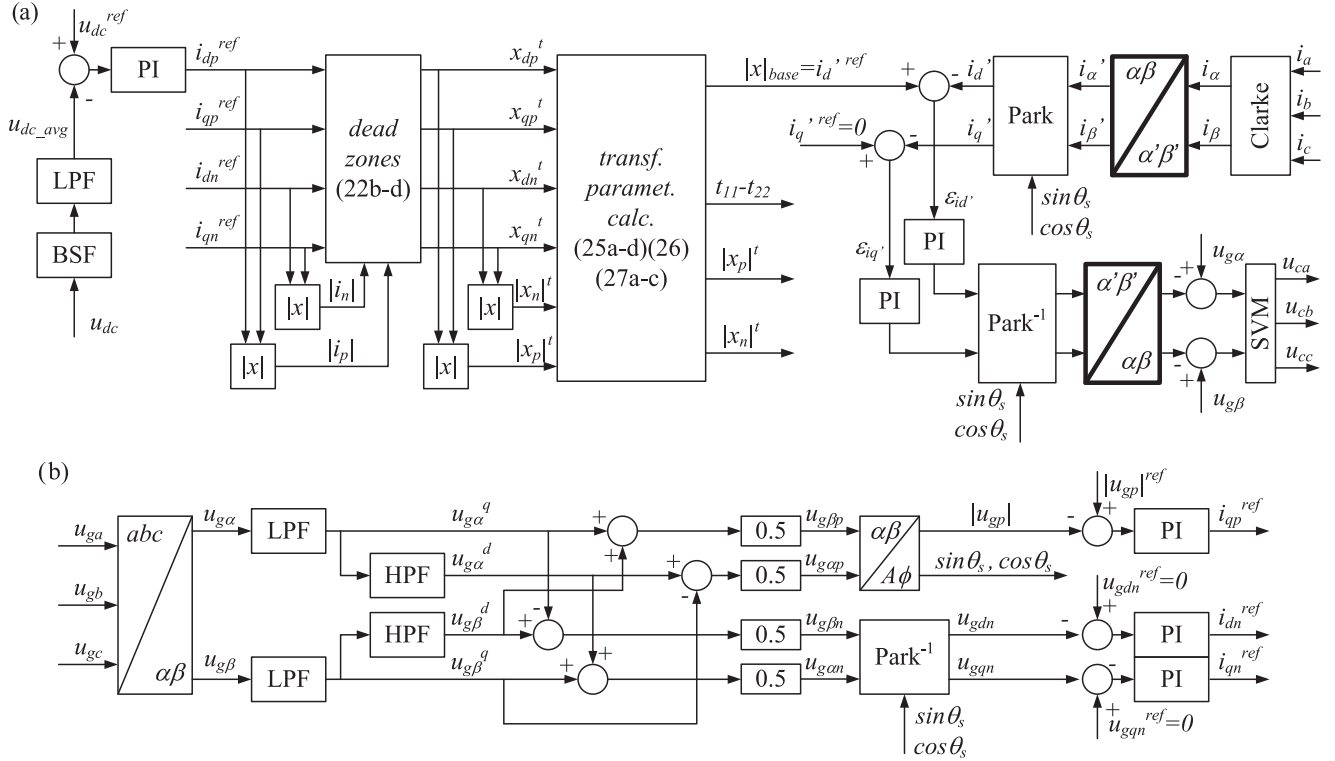
Fig. 5.   Proposed methods of control and calculation of the non-Cartesian frame transformation parameters. a) New transformation parameters calculation and converter current control in the non-Cartesian frame. b) Example method of Park's transformation angle calculation and grid voltage imbalance compensation.

It can be observed that for properly implemented control structures, in all methods, converter current is kept sinusoidal, and in the steady state, no visible differences occur. The DSFR control [see Fig. 6(b)] provides the slowest response due to the use of notch filters in current measurement paths, needed for symmetrical sequences extraction. These filters introduce additional dynamic terms to the control plant seen by the current regulators. Thus, the observed inertia in the response is justified. Elimination of notch filters in DSRF-based control is possible by the implementation of decoupling structures between positive and negative sequences, but the structure becomes more complicated. Slight overregulation in the first period occurs. In both cases of DSFR control, four regulators are responsible for current control and multiple Park's transformations are used. To avoid multiple transformations of positive and negative sequences of current, oscillatory terms are introduced. It gives negligibly better results without overregulation [seeFig. 6(d)].

However, it has to be noted that the oscillatory terms used in the controller structures are problematic in the field of antiwind-up structures used for limitations of the controller's states and their output signals. It requires additional dynamic terms that are difficult to tune. It can be seen in Fig. 6(e) that the proposed method using the new transformation produces comparably good results to the DSFR with positive and negative sequence decoupling as well as to the oscillatory terms based controllers. However, only two controllers are applied here, which facilitates the selection of controller parameters.

The conditions for the second simulation (see Fig. 7) are as follows: positive sequence voltage $|u_p| = 305$ V, negative

sequence voltage $|u_n| = 20$ V , and maximum amplitude from among all phase voltages amplitudes $|u_{abc}|^{\max} = 325$ V, which is also the reference value of the power electronics converter terminal voltage u_{gp}^{ref} for the positive sequence grid voltage amplitude $|u_{gp}|$ regulator. The reference value of dc bus voltage equals 650 V, filter inductance 2 mH, filter inductor resistance 0.1 Ω, grid impedance values are similar, i.e., 2 mH of inductance and 0.5 Ω of resistance.

To speed up the method prototyping in this test, continuous voltage sources were used instead of a switching power converter. The complete results of the switched converter are shown in the section related to the laboratory tests.

Operation of the power converter starts at 0.05 s. The dc bus of the power converter is neither loaded nor the energy is transferred from the external dc source. Thus, in the initially charged dc bus, the dc voltage remains unchanged. At 0.05 s, the power converter terminal voltage imbalance and the positive sequence sag are started to be compensated for. Simultaneously, the dc bus voltage controller starts working. Visible dc bus voltage oscillations are caused by the negative sequence current flow influencing the instantaneous power p component.

At 0.3 s, the dc bus starts to fed by the external constant current source equal to 40 A, which for the average dc bus voltage equal to 650 V is equivalent to 26 kW of power. It can be observed that in the steady state both new i_d' and i_q' current components as well as output signals of the current regulators $outRi_d'$ and $outRi_q'$ are constant. It proves that the presented concept can be of interest in grid-connected power converter control as it allows to eliminate positive and negative sequence extraction as well
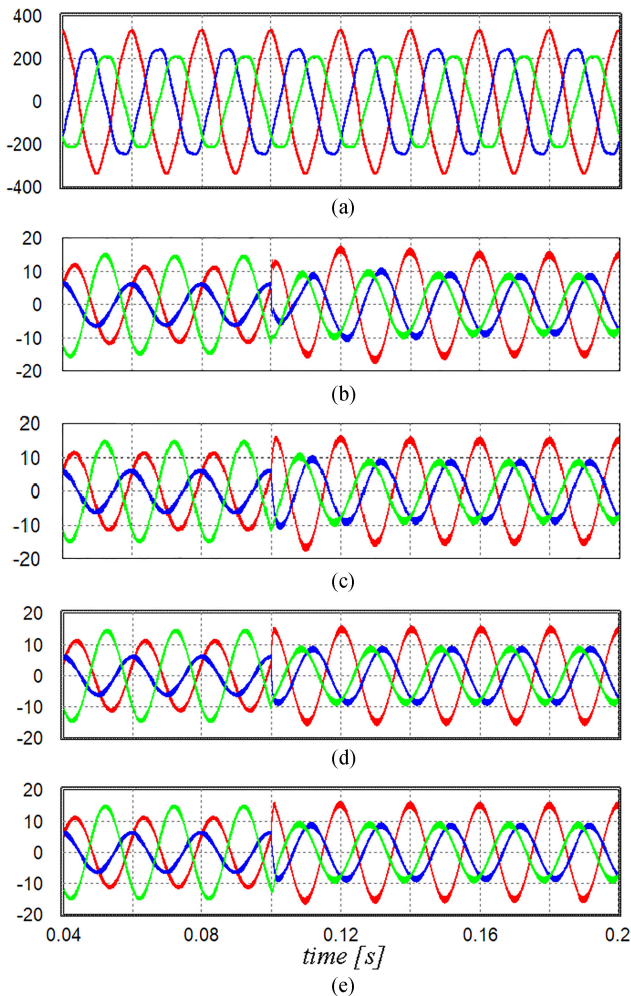
Fig. 6. (a) Simulation results presenting three-phase grid voltage. (b) Three-phase unbalanced current for DSFR control with notch filters. (c) DSFR control with positive and negative sequence decoupling. (d) Oscillatory terms based current controllers. (e) Proposed current control method during reference step change of the converter current imbalance.

TABLE I
PARAMETERS OF THE POWER CONVERTER USED IN THE LABORATORY

Symbol	PARAMETER	Value
U_{gn}	Nominal phase voltage (L-N rms)	133V
I_n	Rated current rms	14A
L	Grid filter inductance	1.2mH
R_L	Inductor resistance	40mΩ
C_{dc}	dc link capacitance	1mF
f_s	Switching frequency	10kHz

as resonant terms in the current controller structures for which the antiwind-up structure is not as trivial and intuitive as for the PI term.

V. EXPERIMENTAL TESTS OF CONTROL METHODS WITH NON-CARTESIAN FRAME TRANSFORMATION

Experimental tests were done with a 5.5-kW converter. The converter parameters are provided in Table I.

Fig. 8 presents experimental tests for arbitrarily referenced positive and negative sequence current vector components at some asymmetry of the grid voltage in the inverter operation mode. The grid impedance in this test is considerably low and the grid converter current has no influence on the grid voltage. This is to show that it is possible to obtain sinusoidal unbalanced current of given asymmetry different than grid voltage asymmetry. At the beginning, the positive sequence current is fed only, while at the end of the test, the negative sequence current is fed only. In the middle part of the test, the converter current vector crosses the dead zone.

Fig. 9 presents a similar test over a longer time. Here, at the beginning of the test only a negative sequence current is delivered to the grid, whereas positive sequence current is delivered at the end. This can easily be identified through observation of the dc bus voltage oscillations which are negligible for positive sequence current and considerable for negative sequence current. Fig. 9 also presents hodographs of the current vector in the natural stationary frame and in the new oblique stationary frame. Small disturbances of the circular hodograph in a new frame are visible due to the transients caused by crossing the dead zone.

The second set of experimental tests was done for rectifier operation with implemented outer control loops related to the dc bus voltage regulation through positive sequence *d* component of the current vector, the ac voltage amplitude regulation positive sequence *q* component of the current vector, and voltage imbalance compensation through *dq* negative sequence current vector components according to the control scheme in Fig. 5.

Contrary to the previous experiments from Figs. 8 and 9, in these tests, considerably high grid impedance is used (10 mH) to make any influence of the small power converter on the grid voltage possible. Simultaneously, the single-phase significant overload is created on the star-connected windings of the transformer which is used as the grid emulator in the laboratory tests. In the first test from Fig. 10, the transient of unbalanced voltage sag is shown at power rectifier operating with disabled negative sequence grid voltage regulators and with arbitrarily zeroed negative sequence reference current vector components. For the grid voltage sag, the positive sequence current is increased to satisfy the dc load energy demand, which is unchanged due to the same dc voltage value.

In the second test from Fig. 11, the grid voltage imbalance regulators (correctors) are enabled and after a short time the grid voltage is recovered in each phase due to delivery of an adequate amount of negative sequence in the converter current. The response of the system in Fig. 11 is not immediate due to the existing filters in the dc and ac voltage outer control loops and high capacitance of the dc bus.

However, the new transformation in the inner control loop does not introduce extra dynamics, as can be observed in Fig. 12 which presents the current control loop step response to arbitrarily referenced current imbalance change. The test was done for the same high grid impedance. High impact of negative sequence current on grid voltage imbalance can be observed. The last test was provided for an enormous amount of harmonics in the grid voltage (Fig. 13).
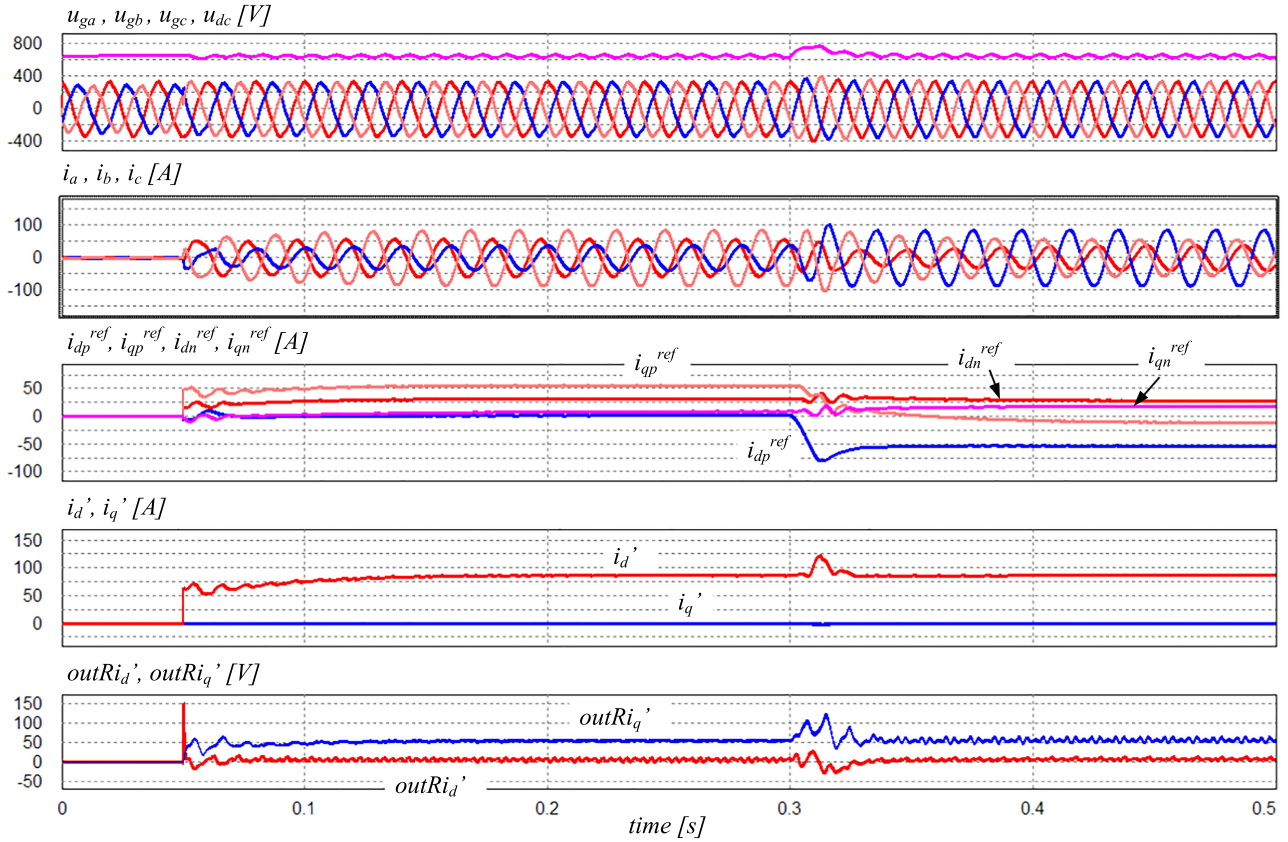
Fig. 7. Simulation results presenting operation of the grid power converter with the application of new transformations for the case of grid voltage imbalance compensation and fundamental positive sequence component sag compensation (0–0.05 s – initial state, 0.05–0.3 s – no load operation with imbalance and sag compensation, 0.3–0.5 s – imbalance and sag compensation with simultaneous dc bus feeding from external source by 26 kW of power (inverter operation mode).
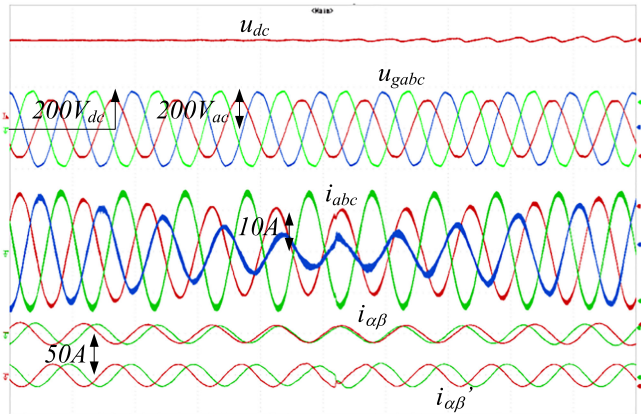

Fig. 8. Experimental results of short time transient of progressive change from positive sequence current referencing to negative sequence current referencing (u_{dc} – dc bus voltage, u_{sabc} – three-phase grid voltage, i_{abc} – three-phase converter current, $i_{\alpha\beta}$ – converter current components in the natural stationary frame, $i_{\alpha\beta}'$ – converter current components in a new stationary frame).
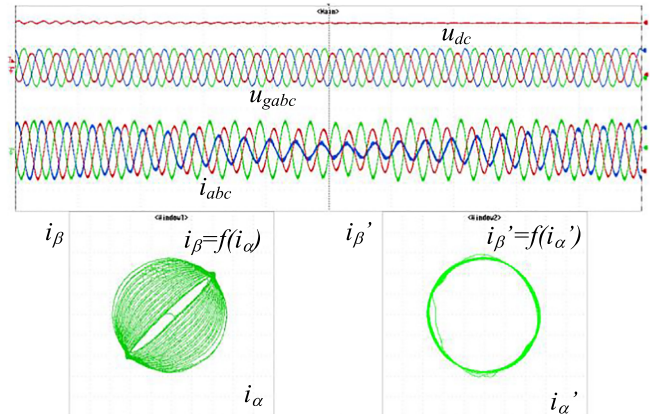

Fig. 9. Experimental results of long time transient of progressive change from negative sequence current referencing to positive sequence current referencing (u_{dc} – dc bus voltage, u_{sabc} – three-phase grid voltage, i_{abc} – three-phase converter current, $i_\beta = f(i_\alpha)$ – converter current hodograph in the natural stationary frame, $i_\beta' = f(i_\alpha')$ – converter current hodograph in a new frame).

The last test was provided for an enormous amount of harmonics in the grid voltage. The grid voltage is distorted by a six-pulse three-phase diode rectifier connected in parallel to the tested converter terminals. Thus, besides already existing harmonics and intentionally provided unbalanced grid voltage sag, additional harmonics are generated. Independent of that,

the converter current keeps sinusoidal shape and performs its function as a grid voltage imbalance compensator.

As the proposed solution of the power converter is not intended to be used as an active power filter, the intentional converter current harmonics are not taken into consideration. Although special transformation giving constant signals in
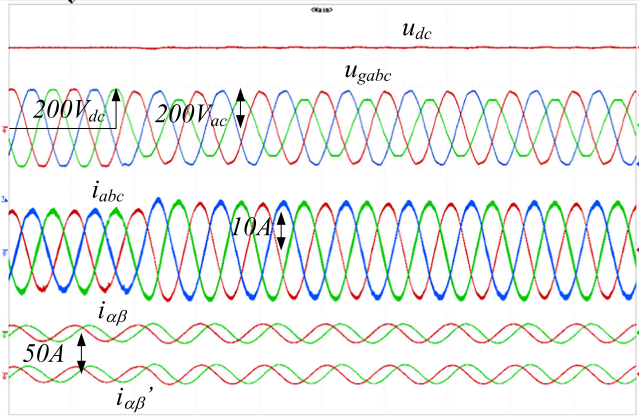
Fig. 10. Experimental results during transient of unbalanced grid voltage sag with disabled negative sequence grid voltage regulators (u_{dc} – dc bus voltage, u_{sabc} –three-phase grid voltage, i_{abc} –three-phase converter current, $i_{\alpha\beta}$ – converter current components in the natural stationary frame, $i_{\alpha\beta}'$ – converter current components in a new stationary frame).
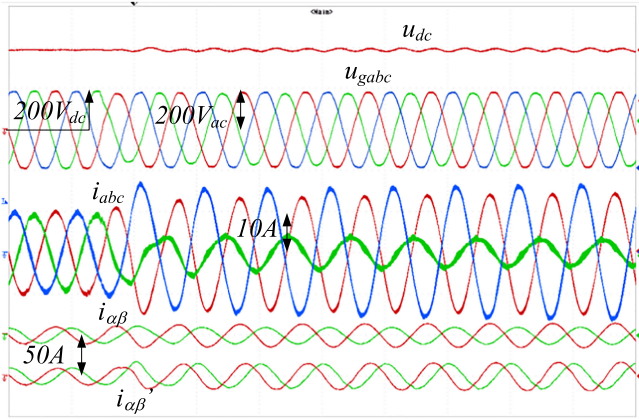

Fig. 11. Experimental results during transient of unbalanced grid voltage sag with enabled negative sequence grid voltage regulators (u_{dc} – dc bus voltage, u_{sabc} –three-phase grid voltage, i_{abc} – three-phase converter current, $i_{\alpha\beta}$ – converter current components in the natural stationary frame, $i_{\alpha\beta}'$ – converter current components in a new stationary frame).

Fig. 12. Experimental results of step response of current control loop to arbitrarily changed reference current imbalance (u_{dc} – dc bus voltage, u_{sabc} –three-phase grid voltage, i_{abc}-three-phase converter current, $i_{\alpha\beta}$ – converter current components in the natural stationary frame, $i_{\alpha\beta}'$ – converter current components in a new stationary frame).
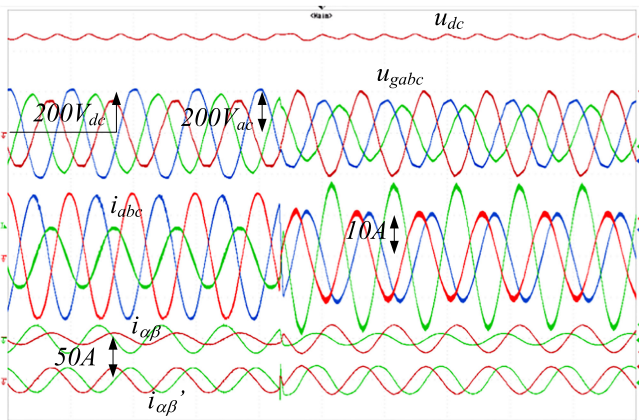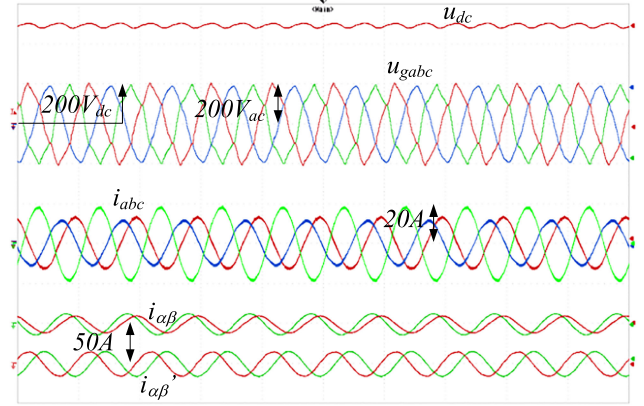

Fig. 13. Experimental results of grid voltage imbalance compensation at enormously high content of grid voltage harmonics (u_{dc} – dc bus voltage, u_{sabc}-three-phase grid voltage, i_{abc} – three-phase converter current, $i_{\alpha\beta}$ – converter current components in the natural stationary frame, $i_{\alpha\beta}'$ – converter current components in the new stationary frame).

synchronously oriented frame was elaborated [24], until now it was utilized for improvement of the phase locked loop response. Further studies are needed on implementation of this or similar concept for intentional introduction of converter current harmonics without implementation of a multiple reference frame or multiresonant current controllers.

VI. CONCLUSION

The article presents a new transformation of unbalanced three-phase signals to the oblique non-Cartesian frame in which the obtained signals in the new frame have equal amplitudes and are shifted by $\pi/2$ despite three-phase signals imbalance. Thus, in a new frame, the vector is seen as balanced. Transformed next to the rotating frame using Park's transformation, the vector components are constant. The proposed transformation from stationary $\alpha\beta$ to new $\alpha'\beta'$ frame and next from $\alpha'\beta'$ to the $d'q'$ frame was used in the voltage-oriented vector control of a three-phase grid converter.

The new transformation parameters can be relatively simply found based on reference positive and negative sequence current vector components, making it possible to obtain any imbalance of converter current depending on the outer control loops referencing current vector components.

The method has a limitation in a narrow range of current asymmetries, where the magnitude of positive sequence vector is close to the magnitude of the negative sequence vector, therefore, a dead zone is implemented to avoid converter operation in this narrow range. Simulation and experimental results show that the method works in a stable manner even when crossing the dead zone. Simulation and experimental tests were done with disabled outer control loops of dc and ac voltage (so with arbitrarily referenced positive and negative sequence components) and with enabled outer control loops. In both cases, the results are satisfactory.

APPENDIX

REPRESENTATION OF REFERENCE VECTOR IN A NEW FRAME

Taking into account (6) and (12), the basic form of transformations set (11) can be derived as (28).

$$
\begin{bmatrix} x'_d \\ x'_q \end{bmatrix} = \frac{|x|_{\text{base}}}{|x_{\mathrm p}|^2 - |x_{\mathrm n}|^2} \begin{bmatrix} -\frac{x_{\alpha p}}{|x_p|} & \frac{x_{\beta p}}{|x_p|} \\ -\frac{x_{\beta p}}{|x_p|} & \frac{x_{\alpha p}}{|x_p|} \end{bmatrix} \begin{bmatrix} x_{dp} - x_{dn} & x_{qp} - x_{qn} \\ -x_{qp} - x_{qn} & x_{dp} + x_{dn} \end{bmatrix} \begin{bmatrix} (x_{dp} + x_{dn})\frac{x_{\alpha p}}{|x_p|} - (x_{qp} - x_{qn})\frac{x_{\beta p}}{|x_p|} \\ (x_{dp} - x_{dn})\frac{x_{\beta p}}{|x_p|} + (x_{qp} + x_{qn})\frac{x_{\alpha p}}{|x_p|} \end{bmatrix}
$$

$$
= \frac{|x|_{\text{base}}}{|x_p|^2 \left(|x_p|^2 - |x_n|^2\right)} \begin{bmatrix} x_{\alpha p} & x_{\beta p} \\ -x_{\beta p} & x_{\alpha p} \end{bmatrix} \times
$$

$$
\begin{bmatrix} \left(x_{dp}^2 - x_{dn}^2\right) x_{\alpha p} - (x_{dp}x_{qp} - x_{dp}x_{qn} - x_{dn}x_{qp} + x_{dn}x_{qn}) x_{\beta p} + (x_{qp}x_{dp} - x_{qp}x_{dn} - x_{qn}x_{dp} + x_{qn}x_{dn}) x_{\beta p} + \left(x_{qp}^2 - x_{qn}^2\right) x_{\alpha p} \\ (-x_{qp}x_{dp} - x_{qp}x_{dn} - x_{qn}x_{dp} - x_{qn}x_{dn}) x_{\alpha p} + \left(x_{qp}^2 - x_{qn}^2\right) x_{\beta p} + \left(x_{dp}^2 - x_{dn}^2\right) x_{\beta p} + (x_{dp}x_{qp} + x_{dp}x_{qn} + x_{dn}x_{qp} + x_{dn}x_{qn}) x_{\alpha p} \end{bmatrix}
$$

$$
= \frac{|x|_{\text{base}}}{|x_{\mathrm p}|^2 \left(|x_{\mathrm p}|^2 - |x_{\mathrm n}|^2\right)}
$$

$$
\begin{bmatrix} x_{\alpha p} & x_{\beta p} \\ -x_{\beta p} & x_{\alpha p} \end{bmatrix} \begin{bmatrix} \left(|x_p|^2 - |x_n|^2\right) x_{\alpha p} \\ \left(|x_p|^2 - |x_n|^2\right) x_{\beta p} \end{bmatrix} = \frac{|x|_{\text{base}}}{|x_p|^2} \begin{bmatrix} x_{\alpha p}^2 + x_{\beta p}^2 \\ -x_{\beta p}x_{\alpha p} + x_{\alpha p}x_{\beta p} \end{bmatrix} = \begin{bmatrix} |x|_{\text{base}} \\ 0 \end{bmatrix} \tag{28}
$$

REFERENCES

[1] VDE–AR–N 4120: Technical requirements for the connection and operation of customer installations to the high–voltage network VDE, Jan. 2015, Germany.

[2] M. M. Baggu, B. H. Chowdhury, and J. W. Kimball, "Comparison of advanced control techniques for grid side converter of doubly-fed induction generator back-to-back converters to improve power quality performance during unbalanced voltage dips," *IEEE J. Emerg. Sel. Topics Power Electron.*, vol. 3, no. 2, pp. 516–524, Jun. 2015.

[3] W. Liu, F. Blaabjerg, D. Zhou, and S. Chou, "Modified instantaneous power control with phase compensation and current-limited function under unbalanced grid faults," *IEEE J. Emerg. Sel. Topics Power Electron.*, vol. 9, no. 3, pp. 2896–2906, Jun. 2021.

[4] Y. Du, X. Lu, H. Tu, J. Wang, and S. Lukic, "Dynamic microgrids with self-organized grid-forming inverters in unbalanced distribution feeders," *IEEE J. Emerg. Sel. Topics Power Electron.*, vol. 8, no. 2, pp. 1097–1107, Jun. 2020.

[5] A. Mora, R. Cárdenas, M. Urrutia, M. Espinoza, and M. Díaz, "A vector control strategy to eliminate active power oscillations in four-leg grid-connected converters under unbalanced voltages," *IEEE J. Emerg. Sel. Topics Power Electron.*, vol. 8, no. 2, pp. 1728–1738, Jun. 2020.

[6] X. Q. Guo, Y. Yang, and X. Zhang, "Advanced control of grid-connected current source converter under unbalanced grid voltage conditions," *IEEE Trans. Ind. Electron.*, vol. 65, no. 12, pp. 9225–9233, Dec. 2018.

[7] M. Reyes, P. Rodriguez, S. Vazquez, A. Luna, R. Teodorescu, and J. M. Carrasco, "Enhanced decoupled double synchronous reference frame current controller for unbalanced grid-voltage conditions," *IEEE Trans. Power Electron.*, vol. 27 no. 9, pp. 3934–3943, Sep. 2012,

[8] S. Zhou, J. Liu, L. Zhou, and H. She, "Dual sequence current controller without current sequence decomposition implemented on DSRF for unbalanced grid voltage conditions," in *Proc. IEEE Energy Convers. Congr. Expo.*, 2014, pp. 60–67.

[9] A. Milicua, G. Abad, and M. A. Rodriguez Vidal, "Online reference limitation method of shunt-connected converters to the grid to avoid exceeding voltage and current limits under unbalanced operation—Part I: Theory," *IEEE Trans. Energy Convers.*, vol. 30, no. 3, pp. 852–863, Sep. 2015.

[10] G. Iwanski, T. Luszczyk, and M. Szypulski, "Virtual-torque-based control of three-phase rectifier under grid imbalance and harmonics," *IEEE Trans. Power Electron.*, vol. 32, no. 9, pp. 6836–6852, Sep. 2017.

[11] G. Iwanski, "Virtual torque and power control of a three-phase converter connected to an unbalanced grid with consideration of converter current constraint and operation mode," *IEEE Trans. Power Electron.*, vol. 34, no. 4, pp. 3804–3818, Apr. 2019.

[12] A. G. Yepes, F. D. Freijedo, O. Lopez, and J. Doval-Gandoy, "High-performance digital resonant controllers implemented with two integrators," *IEEE Trans. Power Electron.*, vol. 26, no. 2, pp. 563–576, Aug. 2011.

[13] M. Rizo, A. Rodríguez, F. J. Rodríguez, E. Bueno, and M. Liserre, "Different approaches of stationary reference frames saturators," in *Proc. 38th Annu. Conf. IEEE Ind. Electron. Soc.*, Oct. 2012, pp. 2245–2250.

[14] M. Szypulski and G. Iwanski, "Sensorless state control of stand-alone doubly fed induction generator supplying nonlinear and unbalanced loads," *IEEE Trans. Energy Convers.*, vol. 31, no. 4, pp. 1530–1538, Dec. 2020.

[15] Y. Peng, D. Varancic, R. Hanus, and S. Weller, "Anti-windup designs for multivariable controllers," *Automatica*, vol. 34, no. 12, pp. 1559–1565, Dec. 1998.

[16] A. S. Abdel-Khalik, M. S. Hamad, A. M. Massoud, and S. Ahmed, "Post-fault operation of a nine-phase six-terminal induction machine under single open-line fault," *IEEE Trans. Ind. Electron.*, vol. 65, no. 2, pp. 1084–1096, Feb. 2018.

[17] X. Zhou, J. Sun, H. Li, and X. Song, "High performance three-phase PMSM open-phase fault-tolerant method based on reference frame transformation," *IEEE Trans. Ind. Electron.*, vol. 66, no. 10, pp. 7571–7580, Oct. 2019.

[18] T. Guangjun, J. Cheng, and X. Sun, "Tan-Sun coordinate transformation system theory and applications for three-phase unbalanced power systems," *IEEE Trans. Power Electron.*, vol. 32, no. 9, pp. 7352–7380, Sep. 2017.

[19] T. Guangjun and X. Sun, "Analysis of Tan-Sun coordinate transformation system for three-phase unbalanced power system," *IEEE Trans. Power Electron.*, vol. 33, no. 6, pp. 5386–5400, Jun. 2018.

[20] G. Iwanski, P. Maciejewski, and T. Łuszczyk, "New stationary frame transformation for control of a three-phase power converter under unbalanced grid voltage sags," *IEEE J. Emerg. Sel. Topics Power Electron.*, vol. 9, no. 4, pp. 4432–4446, Aug. 2021.

[21] E. Clarke, *Circuit Analysis of AC Power Systems–Symmetrical and Related Components*. Hoboken, NJ, USA: Wiley, 1943, vol. I.

[22] R. H. Park, "Two-reaction theory of synchronous machines generalized method of analysis-part I," *Trans. Amer. Inst. Elect. Eng.*, vol. 48, no. 3, pp. 716–727, Jul. 1929.

[23] G. Iwański, P. Maciejewski, and T. Łuszczyk, "Non-cartesian frame transformation-based control of a three-phase power converter during unbalanced voltage dip – Part I: Transformation principles," *Power Electron. Drives*, vol. 4, no. 39, pp. 1–15, 2019.

[24] G. Tan, C. Zong, and X. Sun, "Tan-Sun transformation-based phase-locked loop in detection of the grid synchronous signals under distorted grid conditions," *Electronics*, vol. 9, no. 4, Apr. 2020, Art. no. 674.

Grzegorz Iwanski (Senior Member, IEEE) received the M.Sc. degree in automatic control and robotics and the Ph.D. degree in electrical engineering from the Faculty of Electrical Engineering, Warsaw University of Technology (WUT), Warsaw, Poland, in 2003 and 2005, respectively.

From 2006 to 2008, he was a Research Worker involved in an international project within the Sixth Framework Programme of the European Union. Since 2009, he has been an Assistant Professor with the Institute of Control and Industrial Electronics, WUT, where he became an Associate Professor in 2019. In 2012–2013, he joined the Renewable Electrical Energy System Team, Universitat Politècnica de Catalunya, Barcelona, Terrassa, Spain, within the framework of the scholarship of Polish Minister of Science and Higher Education. He has coauthored one monograph, three book chapters, and about 80 journal articles and conference papers. He teaches courses on power electronics, drives, and power conversion systems. His research interests include variable and adjustable speed power generation systems, photovoltaics and energy storage systems, and automotive power electronics and drives.

Dr. Iwanski provided two plenary lectures on IEEE technically sponsored international conferences: Ecological Vehicles and Renewable Energies and Joint International Conference on Optimization of Electrical and Electronic Equipment and Aegean Conference on Electrical Machines and Power.

Sebastian Wodyk received the M.Sc. degree in electrical engineering, in 2018, from the Faculty of Electrical Engineering, Warsaw University of Technology, Warszawa, Poland, where he is currently working toward the Ph.D. degree in automation and robotics.

His research interests include control systems of grid-connected power converters and electrical energy storage systems for renewable energy sources and electrical vehicles.

Tomasz Łuszczyk received the M.Sc. and Ph.D. degrees in electrical engineering from Faculty of Electrical Engineering at Warsaw University of Technology, Warszawa, Poland, in 2011 and 2017, respectively.

Since 2017, he has been an Assistant Professor with Institute of Control and Industrial Electronics, WUT. His research is concentrated on vector control of electic machines and grid converters.